Observation of Zero-Dimensional States in a One-Dimensional Electron Interferometer

Wees, B.J. van; Kouwenhoven, L.P.; Harmans, C.J.P.M.; Williamson, J.G.; Timmering, C.E.; Broekaart, M.E.I.; Foxon, C.T.; Harris, J.J.

Published in:
Physical Review Letters

DOI:
10.1103/PhysRevLett.62.2523

Publication date:
1989

Observation of Zero-Dimensional States in a One-Dimensional Electron Interferometer

B. J. van Wees, L. P. Kouwenhoven, and C. J. P. M. Harmans
Department of Applied Physics, Delft University of Technology, P.O. Box 5046, 2600 GA Delft, The Netherlands

J. G. Williamson, C. E. Timmering, and M. E. I. Broekaart
Philips Research Laboratories, 5600 JA Eindhoven, The Netherlands

C. T. Foxon and J. J. Harris
Philips Research Laboratories, Redhill, Surrey RH1 5HA, United Kingdom
(Received 9 March 1989)

We have studied the electron transport in a one-dimensional electron interferometer. It consists of a disk-shaped two-dimensional electron gas, to which quantum point contacts are attached. Discrete zero-dimensional states are formed due to constructive interference of electron waves traveling along the circumference of the disk in one-dimensional magnetic edge channels. The conductance shows pronounced Aharonov-Bohm–type oscillations, with maxima occurring whenever the energy of a zero-dimensional state coincides with the Fermi energy. Good agreement with theory is found, taking energy averaging into account.

PACS numbers: 72.15.Gd, 72.20.My, 73.20.Dx

Advancing technology has made it possible to study electron transport in systems with reduced dimensionality. The ultimate limit is reached when the electron motion is restricted in all directions, and discrete, zero-dimensional states are formed.[1-3]

An elementary way to study these zero-dimensional (0D) states is to construct a one-dimensional (1D) electron interferometer. It is technologically feasible to fabricate such an interferometer by defining a 1D wire by lateral confinement of the electrons, together with controllable barriers at both ends of the wire.[4] We have taken an alternative approach and have employed the one-dimensional nature of the electron transport along the boundary of a two-dimensional electron gas (2DEG) in high magnetic fields. This transport takes place through magnetic edge channels, which consist of the current-carrying states of each Landau level, which are located at the boundaries of the 2DEG.

By defining a disk in a 2DEG, we have made an interferometer in which 0D states are formed by the constructive interference of electron waves traveling along the circumference of the disk in one-dimensional edge channels. Quantum point contacts (QPC's), which are attached to the disk, function as barriers with controllable transmission. This device has the additional advantage that the interference can be tuned by the magnetic flux which penetrates the disk.

A system similar to ours, consisting of a 2D quantum dot to which narrow leads are attached, was studied theoretically by Sivan, Imry, and Hartzstein.[5] Its conductance showed Aharonov-Bohm (AB) type oscillations which were attributed to interference of electrons traveling in edge channels. Jain[6] has predicted similar AB-type oscillations in the high-field conductance of narrow rings. van Loosdrecht *et al.*[7] have observed AB-type oscillations in the conductance of a single quantum point contact. They were explained by the partial reflection of edge channels near both the entrance and exit of the QPC. Compared to Ref. 7, our device provides a clear-cut distinction between the barriers where the reflections take place (these are formed by QPC's) and the 1D conductor which carries the current in between the barriers (the latter is formed by a magnetic edge channel inside the disk).

A schematic layout of our device is given in Fig. 1(a). Current (I_1,I_2) and voltage (V_1,V_2) contacts are at-

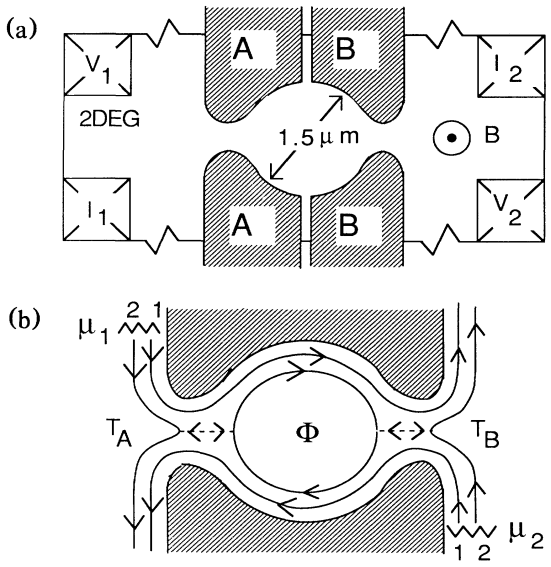

FIG. 1. (a) Layout of the device. (b) Current flow in high magnetic fields. In this example the first edge channel is fully transmitted through the device and the second edge channel forms a one-dimensional interferometer. The interference can be tuned by the flux Φ.

tached to the 2DEG of a high-mobility GaAs/$Al_{0.33}Ga_{0.67}As$ heterostructure. Its electron density is $2.3\times10^{15}/m^2$ and the elastic mean free path is 9 μm. Two gate pairs A and B are defined by electron beam lithography and liftoff techniques. Application of a negative voltage (-0.2 V) to both gate pairs depletes the electron gas underneath the gates. The narrow channels in between the gate pairs are already pinched off at this gate voltage. A disk of 1.5 μm diam is created, which is connected to the wide 2DEG regions by two 300-nm-wide QPC's. A further reduction of the gate voltage widens the depletion regions around the gates. At the QPC's these depletion regions overlap, and a saddle-shaped potential is created, the height of which may be controlled by the gate voltage. Application of a negative voltage to only one gate pair (and zero voltage to the other) also makes it possible to measure the conductances of the individual QPC's, and compare them with the conductance of the complete device.

In high magnetic fields the location of the wave functions of the electrons at the Fermi energy E_F, which constitute the edge channels, is determined by their guiding-center energy E_G:[7,8]

$$E_G = E_F - (n-\tfrac{1}{2})\hbar\omega_c \mp \tfrac{1}{2}g\mu_B B . \quad (1)$$

Electrons with different Landau-level index n and spin orientation flow along different equipotential lines $V(x,y)$, which are determined by the condition $-e\times V(x,y)=E_G$. Figure 1(b) illustrates the electron flow for the case of two occupied (spin-split) Landau levels in the bulk 2DEG. In this example the potential in the QPC's is such that the first edge channel is fully transmitted, and the second edge channel, which follows a different equipotential line, is only partially transmitted through the QPC's. As can be seen in Fig. 1(b), a one-dimensional interferometer is formed by this upper edge channel.

In high magnetic fields the conductances G_A and G_B of QPC's A and B can be written as[9]

$$G_{A,B} = (e^2/h)(N+T_{A,B}) , \quad (2)$$

where N indicates the number of fully transmitted spin-split edge channels and T_A and T_B the partial transmission of the upper edge channel through QPC's A and B. Equation (2) illustrates that in high magnetic fields no scattering between different edge channels takes place in the QPC's.[9] The conductance G_D of the complete device is the sum of the (quantized) conductance of the N fully transmitted edge channels and the conductance of a 1D interferometer:[5,6,10,11]

$$G_D = \frac{e^2}{h}\left[N+\frac{T_A T_B}{1+(1-T_A)(1-T_B)-2[(1-T_A)(1-T_B)]^{1/2}\cos(\theta)}\right] . \quad (3)$$

In this expression θ is the phase acquired by a wave in one revolution around the disk. The relation between this phase and the area A enclosed by the upper edge channel is given by $\theta=2\pi(BA)/\phi_0$, in which $\phi_0=h/e$ is the flux quantum. If T_A and T_B are zero, discrete zero-dimensional states are formed at those energies for which θ equals an integer multiple of 2π. At these energies the edge channel encloses an integer number of flux quanta.[12]

We have measured the conductance of the complete device as well as both individual QPC's as a function of magnetic field. The measurements were performed in a dilution refrigerator, the mixing chamber being at ≈ 6 mK. A lock-in technique was used with a current of 0.5 nA. The gate voltage was fixed at -0.35 V. Increasing the magnetic field has two effects. First, the number of edge channels transmitted through the QPC's is gradually reduced. The conductance of the individual QPC's shows quantized plateaus in those B intervals in which the edge channels are either fully transmitted or completely reflected[9] ($T_A, T_B = 0$). In the intervals between the plateaus the upper edge channel is only partially transmitted ($T_A, T_B \neq 0$). As a second effect, the magnetic field changes the phase θ. Equation (3) predicts that G_D is quantized when both G_A and G_B are quantized, and predicts regular oscillations when G_A and G_B are not quantized, with maxima occurring whenever the energy of a 0D state coincides with the Fermi energy [this implies $\cos\theta=1$ in Eq. (3)].

Figures 2(a) and 2(b) show the measured conductances of the individual QPC's, illustrating the transition from the $3e^2/h$ to the $2e^2/h$ plateau. In contrast to Ref. 7, no oscillations are observed in the individual QPC's. Irregular structure is present instead, with a typical scale of ≈ 0.03 T. This corresponds to one flux quantum in an area of 350×350 nm^2, which is the approximate area of the QPC's. The structure in G_A and G_B can therefore be attributed to random interference effects in the QPC's themselves.

Figure 2(c) shows the conductance of the complete device. Large oscillations are observed, with a period B_0 which slowly varies from 2.5 mT at $B=2.5$ T to 2.8 mT at $B=2.7$ T. As can be seen in Fig. 3(a), which shows them on an expanded scale, these oscillations are extremely regular. The amplitude of the oscillations, as well as their period, does not change significantly when the magnetic field is reversed (and the current and voltage leads are interchanged).[13,14]

Because of the different location of different edge channels [Eq. (1)], they will enclose different areas and their oscillations will therefore have different periods (see below). The observation of a single, well defined period therefore shows that the conductance of only a

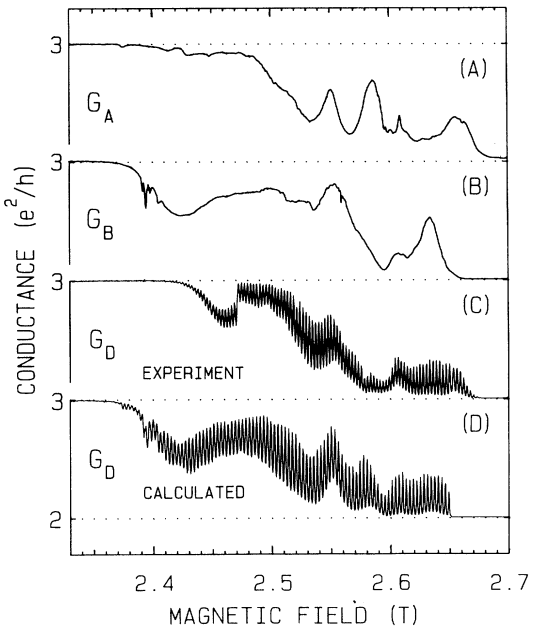

FIG. 2. (a) Conductance G_A of QPC A. (b) Conductance G_B of QPC B. (c) Measured conductance G_D of the complete device. Oscillations occur in the region where both G_A and G_B are not quantized. The maxima occur when the energy of a 0D state coincides with the Fermi energy, due to resonant transmission. (d) Conductance G_D calculated from G_A and G_B with a fixed period $B_0 = 3.0$ mT and $T = 20$ mK.

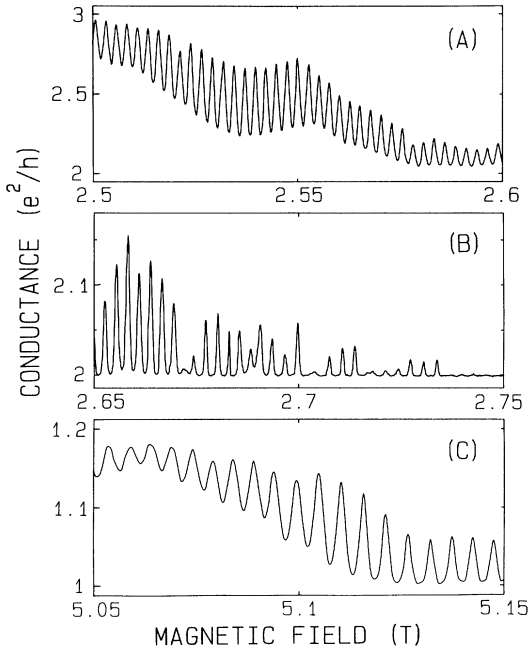

FIG. 3. (a) Measured conductance G_D, showing transmission resonances of the third edge channel. (b) Resonant conductance through zero-dimensional states. In this region the conductance of the third edge channel is almost zero, except when the energy of a 0D state coincides with the Fermi energy. The width of the peaks corresponds with an effective temperature of about 30 mK. (c) Measured conductance G_D, showing transmission resonances due to 0D states belonging to the second edge channel.

single edge channel is modulated. The fact that the conductance in the oscillating region does not drop below $2e^2/h$, nor exceed $3e^2/h$, also shows that a truly one-dimensional interferometer has been realized.

The oscillations disappear when the temperature is raised above 200 mK. They also vanish when the voltage across the device is raised above 40 μV. From this we estimate the energy separation between consecutive 0D states to be about 40 μeV.[15]

Figure 2(d) shows the conductance calculated with Eq. (3). The values for T_A and T_B have been determined from the measured G_A and G_B [Eq. (2)]. A fixed period (3.0 mT) was chosen for the calculations. The finite temperature has been taken into account by including energy averaging: The conductance $G_D(T)$ at finite temperatures is given by $G_D(T) = \int G_D(E)[df(E,T)/dE]dE$, in which $f(E,T)$ is the Fermi distribution function, and $G_D(E)$ is the energy-dependent conductance at zero temperature. The latter can be obtained from Eq. (3) by noting that by changing θ by 2π one obtains the next 0D state, and this corresponds with an energy change of 40 μeV.

Figures 2(c) and 2(d) show a good agreement between the amplitude of the oscillations as well as the amount of modulation, when a temperature of 20 mK is chosen for the calculation. The fact that this temperature is higher than the actual temperature of the device (≈ 6 mK) can be accounted for by the additional energy averaging due to the finite voltage (≈ 6 μV) across the device. This results in an effective temperature $T_e \approx 20$ mK. It was not possible to make a detailed comparison between the structure in G_A and G_B and the structure in G_D. This is probably due to the fact that the application of a voltage to gate pair B results in a slight change in G_A and vice versa.

In the region where T_A and T_B are low, the conductance exhibits very narrow peaks when the energy of a 0D state coincides with E_F, as a result of resonant transmission. This is shown experimentally in Fig. 3(b). Narrow peaks with regular spacing occur in the conductance. Their height is modulated by the structure in G_A and G_B. As a result of the finite effective temperature T_e these peaks are broadened and acquire a half-width of approximately $4kT_e$. From the ratio between half-width and peak spacing (the latter corresponds with an energy of 40 μeV) we obtain $T_e \approx 30$ mK. This is in reasonable agreement with the expected effective temperature of 20 mK resulting from the finite temperature and finite voltage across the device.

Zero-dimensional states belonging to other edge channels have also been observed. Figure 3(c) shows the os-

cillations from the second edge channel. Their period ($B_0=5.3$ mT at $B=5.1$ T) is different from the oscillations from the third edge channel discussed above. Also oscillations from the fourth ($B_0=2.1$ mT at $B=1.85$ T) and fifth edge channels ($B_0=1.4$ mT at $B=1.25$ T) have been observed.

The observed oscillations as a function of magnetic field are different from the Aharonov-Bohm oscillations observed in small metal[16] or semiconductor[17] rings. In our device the edge channels which carry the current are only formed when the magnetic field is applied. A variation of the magnetic field changes the location of these edge channels [Eq. (1)]. The change in enclosed flux $\Delta\Phi$ resulting from the change in field ΔB can now be written as

$$\Delta\Phi=\Delta(B\pi r^2)=\pi r^2\Delta B+B2\pi r\Delta r$$
$$=\left(\pi r^2+\frac{B2\pi r}{eE}\frac{dE_G}{dB}\right)\Delta B. \quad (4)$$

The change in edge channel radius is given by $\Delta r=\Delta E_G/eE$, in which E is the radial electric field at the location of the edge channel. Evaluation of (4) with $r=750$ nm, $B=2.5$ T, and the rough estimate[18] $E=3\times10^4$ V/m shows that the second term (which is negative) can be of the same order as the first one. Therefore, the observed period $B_0=\phi_0\Delta B/\Delta\Phi$ is not simply related to the area enclosed by the edge channel, but depends on the magnetic field and the form of the electrostatic potential in which the electrons are confined.[19]

In summary we have reported a realization of a one-dimensional electron interferometer, in which the discrete electronic states show up in a very pronounced way.

We thank L. W. Molenkamp. A. A. M. Staring, and C. W. J. Beenakker for valuable discussions, S. Phelps at the Philips Mask Centre and the Delft Centre for Submicron Technology for their contribution in the fabrication of the devices, and the Stichting voor Fundamenteel Onderzoek der Materie (FOM) for financial support.

[1]J. Cibert, P. M. Petroff, G. J. Dolan, S. J. Pearton, A. C. Gossard, and J. H. English, Appl. Phys. Lett. **49**, 1275 (1986).

[2]M. A. Reed, J. N. Randall, R. J. Aggarwall, R. J. Matyi, T. M. Moore, and A. E. Wetsel, Phys. Rev. Lett. **60**, 535 (1988).

[3]T. P. Smith, III, K. Y. Lee, C. M. Knoedler, J. M. Hong, and D. P. Kern, Phys. Rev. B **38**, 2172 (1988).

[4]C. G. Smith, M. Pepper, H. Ahmed, J. E. F. Frost, D. G. Hasko, D. C. Peacock, D. A. Ritchie, and G. A. C. Jones, J. Phys. C **21**, L893 (1988).

[5]U. Sivan, Y. Imry, and C. Hartzstein, Phys. Rev. B **39**, 1242 (1989); U. Sivan and Y. Imry, Phys. Rev. Lett. **61**, 1001 (1988).

[6]J. K. Jain, Phys. Rev. Lett. **60**, 2074 (1988).

[7]P. H. M. van Loosdrecht, C. W. J. Beenakker, H. van Houten, J. G. Williamson, B. J. van Wees, J. E. Mooij, C. T. Foxon, and J. J. Harris, Phys. Rev. B **38**, 10162 (1988).

[8]*The Quantum Hall Effect,* edited by R. E. Prange and S. M. Girvin (Springer-Verlag, New York, 1987).

[9]B. J. van Wees, E. M. M. Willems, C. J. P. M. Harmans, C. W. J. Beenakker, H. van Houten, J. G. Williamson, C. T. Foxon, and J. J. Harris, Phys. Rev. Lett. **62**, 1181 (1989).

[10]M. Büttiker, IBM J. Res. Dev. **32**, 63 (1988).

[11]J. K. Jain and S. A. Kivelson, Phys. Rev. Lett. **60**, 1542 (1988).

[12]B. I. Halperin, Phys. Rev. B **25**, 2185 (1982).

[13]Due to a slow drift of the device parameters the fine structure in consecutive traces did not fully reproduce. This prevented a detailed test of the symmetry of the magnetoconductance. However, the amplitude of the oscillations as well as their period were approximately the same for both field orientations.

[14]van Loosdrecht *et al.* (Ref. 7) have observed a large asymmetry in the amplitude of the oscillations in forward and reverse fields. Also, two sets of oscillations with slightly different periods were observed, which were attributed to spin splitting. In our device the spin splitting is fully resolved, as a result of which we only expect and observe a single set of oscillations.

[15]The Fermi energy is ≈9 meV, which means that a large number of 0D states are occupied.

[16]R. A. Webb, S. Washburn, C. P. Umbach, and R. B. Laibowitz, Phys. Rev. Lett. **54**, 2696 (1985).

[17]G. Timp, A. M. Chang, J. E. Cunningham, T. Y. Chang, P. Mankiewich, R. Behringer, and R. E. Howard, Phys. Rev. Lett. **58**, 2814 (1987); C. J. B. Ford, T. J. Thornton, R. Newbury, M. Pepper, H. Ahmed, C. T. Foxon, J. J. Harris, and C. Roberts, J. Phys. C **21**, L325 (1988).

[18]At the 2DEG boundary the electrostatic potential changes by an amount E_F/e (≈9 mV) in a depletion region which is about 300 nm wide. This gives a typical field strength $E\approx3\times10^4$ V/m.

[19]In a fixed magnetic field (2.5 T) oscillations in G_D are observed with a period ≈1 mV, when the voltage on both gate pairs is swept. From the dependence of this period on the gate voltage we obtained an estimate for the edge channel radius: $r\approx350$ nm.